J Eng Math (2009) 64:251–268
DOI 10.1007/s10665-008-9262-y

Transient dynamics of a rotating spherical liquid drop

Channarong Asavatesanupap · S. S. Sadhal

Received: 20 June 2007 / Accepted: 13 November 2008 / Published online: 6 December 2008

Abstract The transient rotation of a liquid drop in an infinite gaseous medium is analyzed for two cases: viscous retardation from constant-speed rotation, and steady-torque start-up with development to the steady state. This situation arises when a levitated liquid drop is rotated with an acoustically applied torque. Subsequent changes in the torque cause transient effects. To understand such a system, the two basic problems of start-up and retardation are studied. The rotational Reynolds number is considered to be low enough so that nonlinear inertial effects may be neglected. The Laplace-transform method is used to deal with the time dependence. Since the fluid velocity has only the azimuthal direction (and the profile is independent of it), and the other angular dependence is factorable as $\sin\theta$, the solution turns out to be effectively a two-variable problem in r and t. Nevertheless, the finite mass of the spherical drop and its finite viscosity make it a mathematically challenging problem. Besides the full analytical solution, results are obtained in the limits of a solid sphere, and small time for the liquid drop. In all liquid-drop cases, the results are limited to the drop viscosity being higher than the surrounding region. For several common liquids in a gas, the flow field indicates nearly a solid-sphere like behavior, except at small times in the region near the interface. The deviations from the asymptotic center-point velocity are amplified for illustration.

Keywords Laplace transform · Levitation · Rotating drop · Stokes flow · Transient fluid dynamics

1 Introduction

We have been motivated to study the transient dynamics of a rotating levitated liquid drop as a result of our preliminary study of the fluid dynamics of containerless protein crystal growth [1]. In the study of protein crystal growth, one of the aims is to enhance the crystal quality. Towards attaining this goal, containerless processing presents several advantages. One such system has been developed by Chung and Trinh [2] who have used an electrostastically levitated drop of crystal solution (lysozyme) and rotated it acoustically about a horizontal axis. Such

C. Asavatesanupap
Department of Mechanical Engineering, Faculty of Engineering, Thammasat University, Rangsit Campus,
Klong Luang, Pathumthani 12121, Thailand
e-mail: acharnna@engr.tu.ac.th

S. S. Sadhal (✉)
Department of Aerospace & Mechanical Engineering, University of Southern California, Los Angeles, CA 90089-1453, USA
e-mail: sadhal@usc.edu

a process neutralizes some gravitational effects and proper control of rotational speed can effectively contain the growing crystal within the confines of the solution drop.

Our analytical investigation for the dynamics of a rotating drop containing a solid particle has led us to a more fundamental problem of the transient dynamics of a rotating drop which may be manipulated by altering the intensity of the rotational torque. With the idea of investigating this in more detail, we consider a liquid drop that is experiencing two different transients, one when the torque is turned off, and another when the torque is turned on. In the first case, a drop is initially rotating steadily under the force of a constant but spatially non-uniform torque. Under such circumstances, the drop rotates like a solid body. However, when the torque is turned off, motion within the drop ensues due to the redistribution of shear stress at the drop surface. In the second case, as an initially stationary drop, a torque is applied and the drop begins rotating and eventually achieves the steady state. In such cases, we are interested in determining the flow characteristics within the drop and in understanding the limits of the parameters under which the basic rotation may be regarded as solid-body type for the modeling of the more complex problem of a particle within a rotating drop.

To understand the dynamics, we consider a drop rotating steadily with angular speed, Ω_0; at time $t = 0$ the torque is turned off, causing the drop to begin decelerating. The other end of the problem is the case when drop rotation is started with a constant but non-uniform torque, $\sigma_0 \sin\theta$, and ends up in steady state with a constant rotational speed. Even though in actual experiments the start-up of an acoustic torque causes a more complex flow field [3], our study is just an attempt to understand transients in a more fundamental sense. The results are limited to cases in which the liquid-drop viscosity is higher than that of the surrounding medium.

The studies of a rotating solid sphere go back many decades [4–6]. Among these works, the transient effects have been treated by Ghildyal [6] who analyzed a solid sphere rotating at a constant rotational speed. This is a considerably simpler problem than the current one, considering that both the fluidity of the particle and its finite mass are not factored.

2 Problem statement and method of solution

We consider a liquid drop of radius r_0 levitated in an unbounded gaseous medium and rotating about a horizontal axis with angular velocity Ω_0. In our analysis, the rotation rate is assumed to be sufficiently low for the velocity field in the gaseous medium as well as within the rotating drop to be approximated by a Stokes flow ($\mathrm{Re} \ll 1$). We define the flow Reynolds numbers based on the angular velocity Ω_0 so that $\mathrm{Re} = \Omega_0 r_0^2/\nu \ll 1$ and $\hat{\mathrm{Re}} = \Omega_0 r_0^2/\hat{\nu} \ll 1$. From here on, the hat ($\hat{}$) is used to denote parameters in the liquid phase. We may also define the Ekman number $\mathrm{Ek} = \mathrm{Re}^{-1}$ which represents the ratio of the viscous to the rotational forces. When $\mathrm{Ek} \gg 1$, the Ekman layer is sufficiently thick to allow the fluid flow to have only the ϕ-component of velocity. In a spherical coordinate system, the unsteady Stokes equations governing the system are:

$$\text{Liquid drop:} \quad \frac{\partial \hat{u}_\phi}{\partial t} = \hat{\nu}\left(\nabla^2 \hat{u}_\phi - \frac{\hat{u}_\phi}{r^2 \sin^2\theta}\right), \tag{1a}$$

$$\text{Gaseous environment:} \quad \frac{\partial u_\phi}{\partial t} = \nu\left(\nabla^2 u_\phi - \frac{u_\phi}{r^2 \sin^2\theta}\right). \tag{1b}$$

The initial and boundary conditions depend on whether the problem is for a decelerating drop or a start-up case. Therefore, these are discussed in Sects. 3 and 4, respectively. We now assume that the solutions of (1) may be written as follows

$$\hat{u}_\phi = \hat{u}(r,t)\sin\theta, \tag{2a}$$

$$u_\phi = u(r,t)\sin\theta. \tag{2b}$$

Inserting (2) into (1) and using the Laplace-transform method, one can write the transformed equations as follows:

$$r^2\hat{U}'' + 2r\hat{U}' - \left(\frac{sr^2}{\hat{\nu}} + 2\right)\hat{U} = -\frac{r^2\hat{u}(r,0)}{\hat{\nu}}, \tag{3a}$$

$$r^2U'' + 2rU' - \left(\frac{sr^2}{\nu} + 2\right)U = -\frac{r^2u(r,0)}{\nu}, \tag{3b}$$

where $\hat{U}(r,s) \equiv \mathsf{L}\left\{\hat{u}(r,t)\right\}$ and $U(r,s) \equiv \mathsf{L}\{u(r,t)\}$ denote Laplace transforms. The initial velocities $u(r,0)$ and $\hat{u}(r,0)$ are given in Sects. 3 and 4 for the respective decelerating and start-up cases in terms of $\hat{u}_\phi$ and u_ϕ.The general solution of the set of equations (3) that remains bounded for both media, takes the form

$$\hat{U}(r,s) = \hat{C}_1\left(\frac{e^{(r/r_0)\hat{X}}[(r/r_0)\hat{X}-1] + e^{-(r/r_0)\hat{X}}[(r/r_0)\hat{X}+1]}{r^2}\right) + \frac{\hat{u}(r,0)}{s}, \tag{4a}$$

$$U(r,s) = C_1\left(\frac{e^{-(r/r_0)X}[(r/r_0)X+1]}{r^2}\right) + \frac{u(r,0)}{s}. \tag{4b}$$

where $\hat{X} = \sqrt{s\hat{\tau}}$ and $X = \sqrt{s\tau}$. At this point, we define the dimensionless radial coordinate, $\mathsf{R} = r/r_0$. However, we shall use the notation (r/r_0) for clarity, wherever appropriate. The parameters $\hat{\tau}$ and τ are the diffusion time scales with respect to the kinematic viscosity of liquid drop and gas media, respectively, and can be defined as

$$\hat{\tau} = \frac{r_0^2}{\hat{\nu}} \quad \text{and} \quad \tau = \frac{r_0^2}{\nu}.$$

It should be noted that (4) consists of the homogeneous and particular solutions which correspond to time-dependent and time-independent parts, respectively. The unknown coefficients $\hat{C}_1$ and C_1 must be determined by boundary and interface conditions which will be specified later.

3 Case of a decelerating liquid drop

We begin our analysis with the case in which a liquid drop is initially rotating steadily in a gaseous medium at angular velocity Ω_0. With a steady torque applied on a homogeneous drop, the rotating drop will maintain rotational motion as a solid body in the steady-state situation. The flow field in the gaseous medium is simply given by the steady Stokes-flow solution of a rotating sphere in an infinite medium. The rotating drop is allowed to decelerate by turning off the torque. Thus, the initial and boundary conditions of this problem are given by

$$\hat{u}_\phi = \Omega_0 r\sin\theta, \quad u_\phi = \frac{\Omega_0 r_0^3}{r^2}\sin\theta \quad \text{at } t = 0, \tag{5a}$$

and

$$\hat{u}_\phi = u_\phi, \hat{\sigma}_{r\phi} = \sigma_{r\phi} \quad \text{at } r = r_0, \tag{5b}$$

for which the Laplace transforms are rather straight forward.

The solutions of (4) satisfying the transforms of the conditions (5) are

$$\hat{U}(r,s) = \frac{\Omega_0 r}{s} - \frac{3\delta\Omega_0 r_0^3}{r^2}\left(\frac{(X+1)\{e^{(r/r_0)\hat{X}}[(r/r_0)\hat{X}-1] + e^{-(r/r_0)\hat{X}}[(r/r_0)\hat{X}+1]\}}{s\Delta}\right), \tag{6a}$$

$$U(r,s) = \frac{\Omega_0 r_0^3}{sr^2} - \frac{3\delta\Omega_0 r_0^3}{r^2}\left(\frac{[(r/r_0)X+1][e^{-[(r/r_0)-1]X+\hat{X}}(\hat{X}-1) + e^{-[(r/r_0)-1]X-\hat{X}}(\hat{X}+1)]}{s\Delta}\right). \tag{6b}$$

Here $\Delta = e^{\hat{X}}(c_{11}\hat{X}^3 + c_{12}\hat{X}^2 + c_{13}\hat{X} + c_{14}) - e^{-\hat{X}}(c_{21}\hat{X}^3 + c_{22}\hat{X}^2 + c_{23}\hat{X} + c_{24})$
where

$$\begin{aligned}
c_{11} &= \kappa + \delta\kappa^2, & c_{21} &= \kappa - \delta\kappa^2,\\
c_{12} &= 1 - 3(1-\delta)\kappa - \delta\kappa^2, & c_{22} &= 1 + 3(1-\delta)\kappa - \delta\kappa^2,\\
c_{13} &= 3(1-\delta)(\kappa-1), & c_{23} &= 3(1-\delta)(\kappa+1),\\
c_{14} &= c_{24} = 3(1-\delta), & \delta &= \mu/\hat{\mu}, \quad \kappa = \sqrt{\hat{\nu}/\nu}, \quad \delta\kappa^2 = \rho/\hat{\rho} = \lambda.
\end{aligned}$$

Thus the shear stress in the rotating drop is

$$\hat{S}_{r\phi} = -3\mu\Omega_0\left(\frac{(X+1)\{e^{\hat{X}}[(r/r_0)^2\hat{X}^2 - 3(r/r_0)\hat{X}+3] - e^{-(r/r_0)\hat{X}}[(r/r_0)^2\hat{X}^2+3(r/r_0)\hat{X}+3]\}}{s\Delta}\right). \tag{7}$$

For large s, the transformed equations (6) and (7) can be expanded as an asymptotic series in negative exponentials. The series-expansion equations take the form

$$\hat{U}(r,s) = \frac{\Omega_0 r}{s} - \frac{3\delta\Omega_0 r_0^3}{r^2}\left(\frac{(X+1)\{e^{-(1-r/r_0)\hat{X}}[(r/r_0)\hat{X}-1] + e^{-(1+r/r_0)\hat{X}}[(r/r_0)\hat{X}+1]\}}{s(c_{11}\hat{X}^3 + c_{12}\hat{X}^2 + c_{13}\hat{X} + c_{14})}\sum_{n=0}^{\infty} G(s)^n\right), \tag{8a}$$

$$U(r,s) = \frac{\Omega_0 r_0^3}{sr^2} - \frac{3\delta\Omega_0 r_0^3}{r^2}\left(\frac{[(r/r_0)X+1][e^{-[(r/r_0)-1]X}(\hat{X}-1) + e^{-[(r/r_0)-1]X-2\hat{X}}(\hat{X}+1)]}{s(c_{11}\hat{X}^3 + c_{12}\hat{X}^2 + c_{13}\hat{X} + c_{14})}\sum_{n=0}^{\infty} G(s)^n\right), \tag{8b}$$

and

$$\hat{S}_{r\phi} = -3\mu\Omega_0\left(\frac{(X+1)\{e^{(r/r_0)\hat{X}}[(r/r_0)^2\hat{X}^2 - 3(r/r_0)\hat{X}+3] - e^{-(r/r_0)\hat{X}}[(r/r_0)^2\hat{X}^2+3(r/r_0)\hat{X}+3]\}}{s(c_{11}\hat{X}^3 + c_{12}\hat{X}^2 + c_{13}\hat{X} + c_{14})}\sum_{n=0}^{\infty} G(s)^n\right) \tag{9}$$

where

$$G(s) = e^{-2\hat{X}}\left(\frac{c_{21}\hat{X}^3 + c_{22}\hat{X}^2 + c_{23}\hat{X} + c_{24}}{c_{11}\hat{X}^3 + c_{12}\hat{X}^2 + c_{13}\hat{X} + c_{14}}\right) \quad \text{and } \hat{S}_{r\phi} = \mathsf{L}\{\hat{\sigma}_{r\phi}\}.$$

3.1 Solid-particle limit ($\delta \to 0$)

One can see that, when the ratio of viscosities is zero, the problem is simply that of a solid sphere rotating in an infinite fluid. In the limit of $\delta \to 0$, while holding the densities fixed, we can obtain the velocity field induced by the rotating sphere from (6b) as follows:

$$U(r,s) = \frac{\Omega_0 r_0^3}{sr^2} + \frac{\Omega_0 r_0^3}{r^2}\left([\Omega(s) - s^{-1}]\frac{1+(r/r_0)X}{1+X}e^{-[(r/r_0)-1]X}\right), \tag{10a}$$

where

$$\Omega(s) = \frac{X+1+5\lambda}{X^3 + (1+5\lambda)X^2 + 15\lambda(X+1)},$$

which may be decomposed in the form

$$\Omega(s) = \frac{m+n\mathrm{i}}{X-a-b\mathrm{i}} + \frac{m-n\mathrm{i}}{X-a+b\mathrm{i}} + \frac{p}{X-c}. \tag{10b}$$

Here, λ is the density ratio between gas media and a solid sphere. With the use of standard inversion tables [7], the time-dependent solution of (10) can be obtained for all (r,t) (see Appendix A). The resulting velocity field outside the sphere is given by

$$u(r,t) = \frac{\Omega_0 r_0^3}{r^2}\left(1 + I_1 + I_2\right), \tag{11}$$

where

$$I_1 = \mathsf{L}^{-1}\left(\Omega(s)\frac{1+\mathsf{R}X}{1+X}e^{-(\mathsf{R}-1)X}\right) = I_{11} + I_{12} + I_{13} + I_{14},$$

and

$$I_2 = \mathsf{L}^{-1}\left(\frac{1+\mathsf{R}X}{1+X}\frac{e^{-(\mathsf{R}-1)X}}{s}\right) = \operatorname{erfc}\left(\frac{\mathsf{R}-1}{2\sqrt{t/\tau}}\right) + (\mathsf{R}-1)\operatorname{erfc}\left(\frac{\mathsf{R}-1}{2\sqrt{t/\tau}} + \sqrt{t/\tau}\right)e^{-(1-\mathsf{R}-\frac{t}{\tau})}.$$

Here,

$$I_{11} = \left(\frac{\mathfrak{Re}\{\mathrm{Z}\} + \alpha}{\beta} + p\mathsf{R}\right) \frac{\mathrm{e}^{-\frac{(\mathsf{R}-1)^2\tau}{4t}}}{\sqrt{\pi t/\tau}},$$

$$I_{12} = \left(\frac{1-\mathsf{R}}{1-c} - \frac{\alpha}{\beta}\right) \mathrm{e}^{-(1-\mathsf{R}-\frac{t}{\tau})}\ \mathrm{erfc}\left(\frac{(\mathsf{R}-1)}{2\sqrt{t/\tau}} + \sqrt{t/\tau}\right),$$

$$I_{13} = -c\left(\frac{1-c\mathsf{R}}{1-c}\right) \mathrm{e}^{(\mathsf{R}-1)c+c^2\frac{t}{\tau}}\ \mathrm{erfc}\left(\frac{(\mathsf{R}-1)}{2\sqrt{t/\tau}} + c\sqrt{t/\tau}\right),$$

and

$$I_{14} = -\frac{2}{\beta}\mathfrak{Re}\left\{(a+b\mathrm{i})\ \mathrm{e}^{(a+b\mathrm{i})(\mathsf{R}-1)+(a^2+b^2)\frac{t}{\tau}}\ \mathrm{erfc}\left(\frac{(\mathsf{R}-1)}{2\sqrt{t/\tau}} + (a+b\mathrm{i})\sqrt{t/\tau}\right)\right\},$$

where

$\mathrm{Z} = 2(m+n\mathrm{i})[(a+b\mathrm{i})\mathsf{R}-1][(a-b\mathrm{i})-1]$, $\alpha = 2(\mathsf{R}-1)[m(1-a)-nb]$, $\beta = [(1-a)^2+b^2]$ and $\mathsf{R} = (r/r_0)$.

3.2 Fluid–fluid system: general solution in integral representation

An examination of the set of equations (6) shows that there are several fairly complex terms whose inverse Laplace transforms are not available in the standard tables. We obtain the inverses of such terms by employing a contour integral in the complex plane. The inverse of the first term in each of (6a) and (6b) is simply a time-independent solution while the remaining terms constitute the time-dependent parts. We have

$$\hat{u}(r,t) = \Omega_0 r - \frac{3\delta\Omega_0 r_0^3}{r^2} \int_{\gamma-\mathrm{i}\infty}^{\gamma+\mathrm{i}\infty} \mathrm{e}^{ts}\, \frac{(X+1)\{\mathrm{e}^{(r/r_0)\hat{X}}[(r/r_0)\hat{X}-1] + \mathrm{e}^{-(r/r_0)\hat{X}}[(r/r_0)\hat{X}+1]\}}{s\Delta}\, \mathrm{d}s, \tag{12a}$$

$$u(r,t) = \frac{\Omega_0 r_0^3}{r^2} - \frac{3\delta\Omega_0 r_0^3}{r^2} \int_{\gamma-\mathrm{i}\infty}^{\gamma+\mathrm{i}\infty} \mathrm{e}^{ts}\, \frac{[(r/r_0)X+1][\mathrm{e}^{-[(r/r_0)-1]X+\hat{X}}(\hat{X}-1) + \mathrm{e}^{-[(r/r_0)-1]X-\hat{X}}(\hat{X}+1)]}{s\Delta}\, \mathrm{d}s. \tag{12b}$$

It can be seen that the integrands of (12) have poles and are double-valued at $s = 0$, therefore possessing a branch point there. Using the standard contour integral, one can show that the integration along a small circle around the branch point produces a term such that it cancels out the time-independent solution. Thus, we finally arrive at the following set of results

Flow fields:

$$\hat{u}(r,t) = \frac{3\delta\Omega_0 r_0^3}{\pi r^2} \int_0^\infty \frac{\mathrm{e}^{-t\rho}(\sqrt{\tau\rho}A - B)}{\rho(A^2+B^2)}\{\sin[(r/r_0)(\hat{\tau}\rho)^{1/2}] - (r/r_0)(\hat{\tau}\rho)^{1/2}\cos[(r/r_0)(\hat{\tau}\rho)^{1/2}]\}\mathrm{d}\rho, \tag{13a}$$

$$u(r,t) = \frac{3\delta\Omega_0 r_0^3}{\pi r^2} \int_0^\infty \frac{\mathrm{e}^{-t\rho}(AC - BD)}{\rho(A^2+B^2)}\mathrm{d}\rho; \tag{13b}$$

Shear stress:

$$\hat{\sigma}_{r\phi} = \frac{3\mu\Omega_0 r_0^3}{\pi r^3} \int_0^\infty \frac{\mathrm{e}^{-t\rho}(\sqrt{\tau\rho}A - B)}{\rho(A^2+B^2)}\{[(r/r_0)^2\hat{\tau}\rho - 3]\sin[(r/r_0)\sqrt{\hat{\tau}\rho}] + 3(r/r_0)\sqrt{\hat{\tau}\rho}\cos[(r/r_0)\sqrt{\hat{\tau}\rho}]\}\,\mathrm{d}\rho, \tag{14}$$

where

$A = [(c_{24}+c_{14}) - \hat{\tau}\rho(c_{22}+c_{12})]\sin(\hat{\tau}\rho)^{1/2} - [(c_{23}-c_{13}) - \hat{\tau}\rho(c_{21}-c_{11})](\hat{\tau}\rho)^{1/2}\cos(\hat{\tau}\rho)^{1/2}$,

$B = [(c_{24}-c_{14}) - \hat{\tau}\rho(c_{22}-c_{12})]\cos(\hat{\tau}\rho)^{1/2} + (c_{23}+c_{13}) - \hat{\tau}\rho(c_{21}+c_{11})](\hat{\tau}\rho)^{1/2}\sin(\hat{\tau}\rho)^{1/2}$,

$C = (\cos\theta_2 - \cos\theta_1) + (\sin\theta_2 + \sin\theta_1)\sqrt{\hat{\tau}\rho} + \mathsf{R}\sqrt{\tau\rho}[(\sin\theta_2 - \sin\theta_1) - (\cos\theta_2 + \cos\theta_1)\sqrt{\hat{\tau}\rho}]$,

$D = (\sin\theta_2 - \sin\theta_1) - (\cos\theta_2 + \cos\theta_1)\sqrt{\hat{\tau}\rho} - \mathsf{R}\sqrt{\tau\rho}[(\cos\theta_2 - \cos\theta_1) + (\sin\theta_2 + \sin\theta_1)\sqrt{\hat{\tau}\rho}]$,

with

$\theta_1 = (\mathsf{R}-1)\sqrt{\tau\rho} - \sqrt{\hat{\tau}\,\rho}$ and $\theta_2 = (\mathsf{R}-1)\sqrt{\tau\rho} + \sqrt{\hat{\tau}\,\rho}$ and $\mathsf{R} = (r/r_0)$

3.3 Small-time approximation

The transformed equations (8) and (9) can be inverted term by term to obtain the solutions applicable for small times, i.e., $t \ll \hat{\tau}$. The inverse Laplace-transform procedure adopted here is straightforward, but rather tedious and similar to that of the solid-sphere case. First, each term which contains a ratio of cubic function in series expansion is split into simpler ratios by using partial-fraction expansion. In carrying out this approximation, we keep only two terms in the large-s expansions given by the summations in (8). Then, employing Eqs. A.1, A.2 and A.3 in Appendix A, one obtains the inverses of $\hat{U}(r,s)$, $U(r,s)$ and $\hat{\sigma}_{r\phi}(r,s)$ using the first two terms of the summations in the set. These are given below:

Flow fields:

The drop-interior velocity field is given by

$$\hat{u}(r,t) = \Omega_0 r_0 \left((r/r_0) - \frac{3\delta}{(\delta\kappa^2+\kappa)(r/r_0)^2} \sum_{n=1}^{4} \hat{I}_n^0 - \frac{3\delta(\delta\kappa-1)}{\kappa(\delta\kappa+1)^2(r/r_0)^2} \sum_{n=1}^{8} \hat{I}_n^1 \right), \tag{15a}$$

and in the exterior,

$$u(r,t) = \Omega_0 r_0 \left(\frac{1}{(r/r_0)^2} - \frac{3\delta}{(\delta\kappa^2+\kappa)(r/r_0)^2} \sum_{n=1}^{4} I_n^0 - \frac{3\delta(\delta\kappa-1)}{\kappa(\delta\kappa+1)^2(r/r_0)^2} \sum_{n=1}^{8} I_n^1 \right), \tag{15b}$$

where I_n^0, I_n^1, $\hat{I}_n^0$, and $\hat{I}_n^1$ are long expressions representing various inverses involving the erfc integral (see Appendix A).

Shear stress:

The shear stress is given by

$$\hat{\sigma}(r,t) = \mu\Omega_0 \left(\frac{3}{(\delta\kappa+1)(r/r_0)} \sum_{n=1}^{4} \hat{J}_n^0 + \frac{3(\delta\kappa-1)}{(\delta\kappa+1)^2(r/r_0)} \sum_{n=1}^{8} \hat{J}_n^1 \right), \tag{16}$$

where again, the expressions for $\hat{J}_n^0$ and $\hat{J}_n^1$ are available in Appendix B. Note that the set of coefficients a_m, b_m and c_m in (15) and (16) are introduced during the partial-fraction-expansion process and given in Appendix A.

4 Case of rotation start-up

In this section we consider the case of an initially stationary drop placed under a steady torque with a $\sin\theta$-type distribution. The drop will eventually achieve the steady state and rotate steadily with a constant angular velocity, Ω_0. It should be recognized that acoustic streaming used in drop levitation induces not only the torque in a time-averaged sense but also the internal circulation within a liquid drop with velocity $O(\delta)$. However, the viscosity of a liquid drop is considerably higher than that of a gas medium, i.e., $\delta \ll 1$. Hence the acoustically driven internal circulation is negligibly small in this investigation. Therefore, the appropriate initial and boundary conditions are given by

$$\hat{u}_\phi = 0, \quad u_\phi = 0 \quad \text{at } t = 0, \tag{17a}$$

and

$$\hat{u}_\phi = u_\phi, \quad \hat{\sigma}_{r\phi} - \sigma_{r\phi} = \sigma_0 \sin\theta \quad \text{at } r = r_0. \tag{17b}$$

The solutions of (4) satisfying the conditions (17) or their Laplace transforms are

$$\hat{U}(r,s)=\frac{\sigma_0 r_0^3\delta}{\mu r^2}\left\{\frac{(X+1)\{\mathrm{e}^{(r/r_0)\hat{X}}[(r/r_0)\hat{X}-1]+\mathrm{e}^{-(r/r_0)\hat{X}}[(r/r_0)\hat{X}+1]\}}{s\Delta}\right\}, \tag{18a}$$

$$U(r,s)=\frac{\sigma_0 r_0^3\delta}{\mu r^2}\left\{\frac{[(r/r_0)X+1][\mathrm{e}^{-[(r/r_0)-1]X+\hat{X}}(\hat{X}-1)+\mathrm{e}^{-[(r/r_0)-1]X-\hat{X}}(\hat{X}+1)]}{s\Delta}\right\}. \tag{18b}$$

The shear stress is

$$\hat{S}_{r\phi}=\sigma_0\left(\frac{(X+1)\{\mathrm{e}^{(r/r_0)\hat{X}}[(r/r_0)^2\hat{X}^2-3(r/r_0)\hat{X}+3]-\mathrm{e}^{-(r/r_0)\hat{X}}[(r/r_0)^2\hat{X}^2+3(r/r_0)\hat{X}+3]\}}{s\Delta}\right). \tag{19}$$

In a similar manner, the inverse Laplace transforms of (18) and (19), using the inversion theorem, are given as

$$\hat{u}(r,t)=\frac{\sigma_0 r_0}{\mu}\left(-\frac{r}{3r_0}+\frac{\delta r_0^2}{\pi r^2}\int_0^\infty\frac{\mathrm{e}^{-t\rho}(B-\sqrt{\tau\rho}A)}{\rho(A^2+B^2)}\{\sin[(r/r_0)(\hat{\tau}\rho)^{1/2}]-(r/r_0)(\hat{\tau}\rho)^{1/2}\cos[(r/r_0)(\hat{\tau}\rho)^{1/2}]\}\,\mathrm{d}\rho\right), \tag{20a}$$

$$u(r,t)=\frac{\sigma_0 r_0}{\mu}\left(-\frac{r_0^2}{3r^2}+\frac{\delta r_0^2}{\pi r^2}\int_0^\infty\frac{\mathrm{e}^{-t\rho}(BD-AC)}{\rho(A^2+B^2)}\,\mathrm{d}\rho\right). \tag{20b}$$

However, it is noted that, contrary to the previous case, the first term of the equations which arises from the integration along a small circle around the branch point survives in this case and represents a steady-state solution of problem. The shear-stress distribution within the liquid drop is obtained as

$$\hat{\sigma}_{r\phi}=\frac{\sigma_0 r_0^3}{\pi r^3}\int_0^\infty\frac{\mathrm{e}^{-t\rho}(\sqrt{\tau\rho}A-B)}{\rho(A^2+B^2)}\left\{[(r/r_0)^2\hat{\tau}\rho-3]\sin[(r/r_0)\sqrt{\hat{\tau}\rho}+3(r/r_0)\sqrt{\hat{\tau}\rho}\cos[(r/r_0)\sqrt{\hat{\tau}\rho}]\right\}\mathrm{d}\rho. \tag{21}$$

In (20) and (21), the coefficients A, B, C, and D are those defined in (14).

4.1 Limit of $\delta \to 0$

In the limit of $\delta \to 0$, the problem can be viewed as a solid sphere rotating in an infinite fluid as the result of the applied torque $\sigma_0 \sin\theta$. The velocity field of the ambient fluid is reduced to

$$U(r,s)=\frac{\sigma_0 r_0^3}{\mu r^2}\frac{\mathrm{e}^{-[(r/r_0)-1]X}}{s}\left(\frac{1+(r/r_0)X}{X^3+(1-5\lambda)X^2-15\lambda(X+1)}\right). \tag{22}$$

Similarly, using the partial-fraction expansion procedure, we may write (22) in the form:

$$U(r,s)=\frac{\sigma_0 r_0^3}{\mu r^2}\frac{\mathrm{e}^{-[(r/r_0)-1]X}}{s}\left(\frac{m+n\mathrm{i}}{X-a-b\mathrm{i}}+\frac{m-n\mathrm{i}}{X-a+b\mathrm{i}}+\frac{p}{X-c}\right). \tag{23}$$

Here, a complex conjugate pair $a \pm b\mathrm{i}$ and a real constant c are the roots of the denominator in (22) which is similar to the denominator of $\Omega(s)$ in (10b). The values of m, n and p are, of course, slightly different from those in (10b). The inverse Laplace transform of (23) can be obtained by the use of standard inversion tables and is given by

$$u(r,t)=\frac{\sigma_0 r_0^3}{\mu r^2}(I_1+I_2) \tag{24}$$

where

$$I_1=2\Re\mathrm{e}\left\{\frac{m+n\mathrm{i}}{a+b\mathrm{i}}\left[-\mathrm{erfc}\left(\frac{\mathsf{R}-1}{2\sqrt{t/\tau}}\right)+\mathrm{e}^{-(a+b\mathrm{i})(\mathsf{R}-1)+(a+b\mathrm{i})^2\frac{t}{\tau}}\mathrm{erfc}\left(\frac{\mathsf{R}-1}{2\sqrt{t/\tau}}-(a+b\mathrm{i})\sqrt{t/\tau}\right)\right]\right\},$$

and

$$I_2 = -\frac{p}{c}\,\mathrm{erfc}\left(\frac{\mathsf{R}-1}{2\sqrt{t/\tau}}\right) + \frac{p}{c}\mathrm{e}^{-c(R-1)+c^2\frac{t}{\tau}}\,\mathrm{erfc}\left(\frac{\mathsf{R}-1}{2\sqrt{t/\tau}} - c\sqrt{t/\tau}\right) \quad \text{with} \quad \mathsf{R} = (r/r_0).$$

As mentioned earlier, the start-up problem for a solid sphere was studied in 1960 by Ghildyal [6]. In that work, the problem of a given step-function steady angular velocity was solved. However, in comparison with the current problem, Ghildyal's [6] work corresponds to an infinite moment of inertia of the solid sphere. In the present case, the sphere mass is finite and, therefore, there are added complexities necessitating finding the roots of a cubic equation (denominator of (10b)).

4.2 Small-time approximation

The inversions of (18) and (19) for small time are

$$\hat{u}(r,t) = \frac{\sigma_0 r_0}{\mu}\left(\frac{\delta}{(\delta\kappa^2+\kappa)(r/r_0)^2}\sum_{n=1}^{4}\hat{I}_n^0 + \frac{\delta(\delta\kappa-1)}{\kappa(\delta\kappa+1)^2(r/r_0)^2}\sum_{n=1}^{8}\hat{I}_n^1\right), \tag{25a}$$

$$u(r,t) = \frac{\sigma_0 r_0}{\mu}\left(\frac{\delta}{(\delta\kappa^2+\kappa)(r/r_0)^2}\sum_{n=1}^{4}I_n^0 + \frac{\delta(\delta\kappa-1)}{\kappa(\delta\kappa+1)^2(r/r_0)^2}\sum_{n=1}^{8}I_n^1\right). \tag{25b}$$

The shear stress is

$$\hat{\sigma}(r,t) = \sigma_0\left(-\frac{1}{(\delta\kappa+1)(r/r_0)}\sum_{n=1}^{4}\hat{J}_n^0 + \frac{(1-\delta\kappa)}{(\delta\kappa+1)^2(r/r_0)}\sum_{n=1}^{8}\hat{J}_n^1\right). \tag{26}$$

5 Results and discussion

We have carried out velocity and shear-stress calculations for various sets of parameters. It should be noted that the expressions for the velocity fields of a rotating drop in an infinite fluid are valid only in the low-Reynolds-number approximation. The numerical calculations are presented in this section. In all figures, the results for $t \ll \tau$ are calculated from small-time solutions (faster convergence) and $t > \tau$ from the general solution. For the case $\delta \to 0$ the solid-sphere calculations are used. It is worthwhile discussing the evaluation of the integral-representation solution of such problems. The problem of integral evaluation is not quite as straightforward because of the complexity of the integrand. Since an analytical expression for the integral could not be found, numerical integration is necessary. The integrals in (20) and (21) are along the real ρ-axis, and the respective integrands each contain a complex pole near the real axis close to some point $\rho = \rho_0$. This gives rise to some difficulty in computing the integral since the integrand takes on large values when approaching $\rho = \rho_0$. The location of a nearby pole must be determined and the integration is divided into two parts, $0 \le \rho \le \rho_0$ and $\rho_0 \le \rho < \infty$. The second integral needs to be evaluated by making a change of variable that transforms the infinite range to one that is finite when ρ approaches infinity. Then, the integration is performed using a six-point Newton–Cotes formula [8]. For a small-time solution, the calculation is straightforward because the solutions are expressed explicitly. The results are compared to those of the integral-representation solutions and the full range of solutions can therefore be established.

It is noted that the results presented in this section are in dimensionless form. Here, we choose the following scales: r_0 as length, $\hat{\tau}$ as time, $\Omega_0 r_0$ or $\sigma_0 r_0/\mu$ as velocity, and $3\mu\Omega_0$ or σ_0 as tangential stress.

5.1 Deceleration of a rotating drop

Figure 1 shows the transient flow field of a rotating water drop in a gaseous medium. In the steady-state situation, the tangential stress due to the applied torque is entirely taken up by the outer medium and the drop will rotate like a

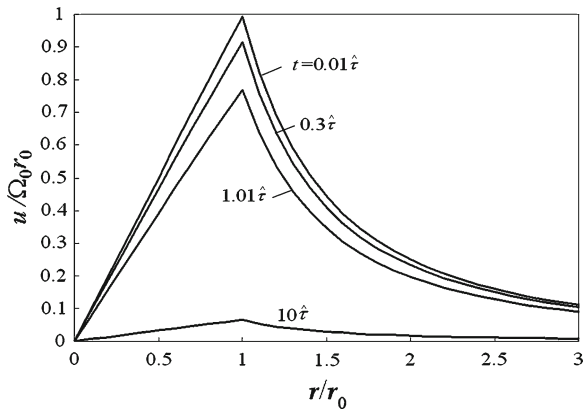

Fig. 1 Velocity fields for a water drop initially rotating with angular velocity Ω_0 in a gas with $\delta = 0.01863$ and $\kappa = 0.25459$

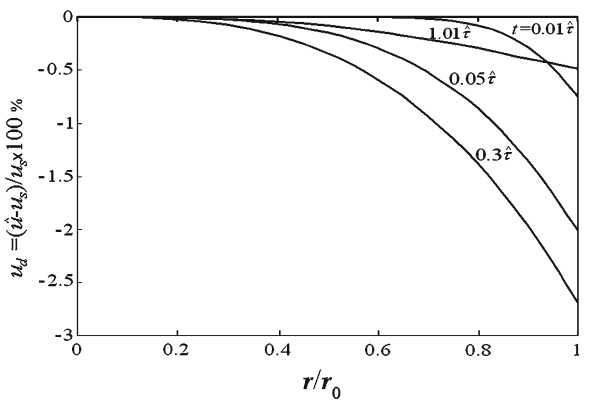

Fig. 2 Scaled deviations of the velocity inside the drop from the solid-body velocity ($\delta = 0.01863$, $\kappa = 0.25459$)

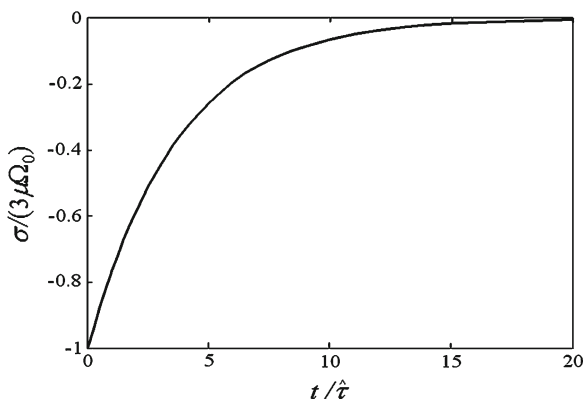

Fig. 3 Interfacial shear stress vs. dimensionless time, $t/\hat{\tau}$

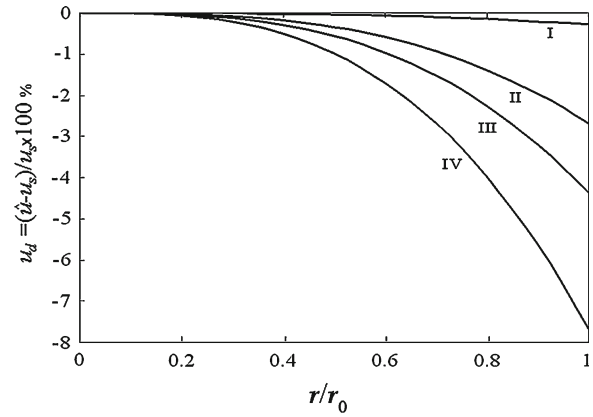

Fig. 4 Scaled velocity deviation from u_s of various liquid drops at $t = 0.3\hat{\tau}$. I: silicone oil, II: water, III: methanol, IV: acetone

solid body. When the applied torque is turned off, the shear stresses at the drop interface starts getting redistributed. The skin friction retards the drop rotation and the angular velocity decreases as time progresses. The velocity is seen to diffuse in time since the system is viscosity-dominated. The exponential character in time with reciprocal of the diffusion time-scale as a factor. As expected, the transient effect initially takes place on the surface from inside and spreads into the drop inside as illustrated in Fig. 2. Here, we plot $u_d = (\hat{u} - u_s)/u_s$, the scaled deviation of the velocity inside the drop from the solid-body velocity, $u_s = \Omega(t)r$. The solid-body velocity used here is not that of the exact solid-sphere case but the velocity defined by the asymptotic value of $\hat{u}$ as $r \to 0$. This is a suitable scaling because the liquid region velocity is nearly equal to this value for short times. It shows that the liquid in the region close to the drop surface is slowed down by surface friction and the region away from the surface still maintains a solid-body-like rotation at $t = 0.01\hat{\tau}$. However, the shear stress gradually penetrates into the center of the drop as illustrated. Consequently, the flow inside the drop starts deviating from the solid-body-like rotation. The largest deviation apparently occurs at the drop surface and reaches a maximum at $t \cong 0.3\hat{\tau}$, approximately. Thereafter, the shear stress inside the drop is slowly depleted as the transient effect dies down. The velocity profile deviates from solid-body rotation less than 0.5% for $t > 1.01\hat{\tau}$. The interfacial shear stress is shown in Fig. 3. The shear stress is seen to decrease monotonically with increasing time and becomes insignificant for $t > 20\hat{\tau}$.

Table 1 Parameters of various liquid drops in air (at 20°C)

Fluid	ν (m^2/s)	ν (m^2/s)	κ	δ
Silocone oil, I	1.02016×10^{-5}	0.003194	0.81352	0.00192
Water, II	0.09720×10^{-5}	0.000986	0.25459	0.01863
Methanol, III	0.07459×10^{-5}	0.000864	0.22274	0.03070
Acetone, IV	0.04150×10^{-5}	0.000644	0.16616	0.05517

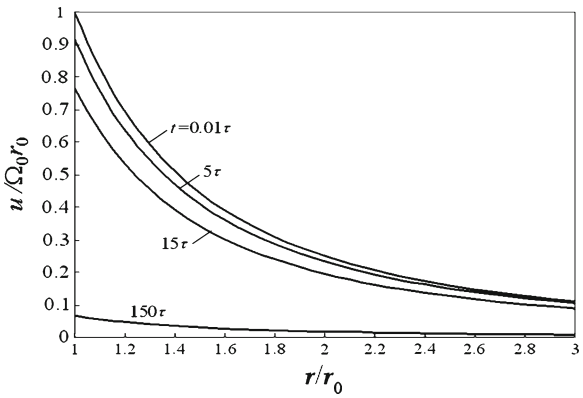

Fig. 5 Velocity field in gaseous medium induced by a freely rotating solid sphere ($\lambda = 0.0012$)

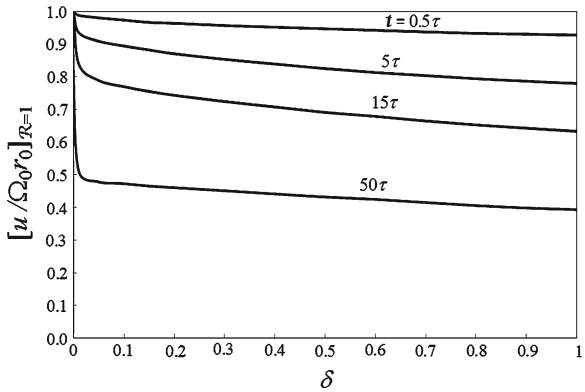

Fig. 6 Dimensionless velocity at the interface as a function of the viscosity ratio δ for $\lambda = 0.001$ at various times

In addition, various liquids in a wide range of viscosities (which are shown in Table 1) were considered as numerical examples and the results are shown in Fig. 4. The results are based entirely on the analytical results obtained with numerical calculations. One can see that the deviation of the flow inside fluid I is much smaller than those of other liquids. This is due to the fact that the viscosity of fluid I is relatively high and therefore the transient effect is suppressed. In contrast, the liquid with low viscosity such as fluid III and fluid IV is notably influenced by the transient effect. The surface stresses penetrate into the drop and the deviation of flow inside the drop is comparatively large. At moderate viscosity, such as that of fluid II, the maximum deviation is approximately 3%. Therefore the solid-body-like rotation approximation is fairly reasonable, especially for high viscous liquid drops, even though the flow at transient state is still affected by the skin friction.

For the solid-sphere case, when turning off the applied torque, the sphere rotates freely and the rotational rate decreases gradually due to surface tangential stresses. With a density ratio $\lambda = 0.0012$, the flow field induced by the freely rotating sphere is shown in Fig. 5. To obtain more insight into the interplay of the various parameters, we have plotted in Fig. 6 the velocity at the interface for constant λ (density ratio) while varying the viscosity ratio δ for various values of the time. The results show a steady decrease of the interfacial velocity with increasing δ. The results are limited to $\delta < 1$ which is based on practical considerations for the system which motivated us to study the problem in the first place. Additionally, for $\delta > 1$, for the mathematical character of the solution changes to discrete poles when carrying out the inverse Laplace transform, and therefore, this range was not tackled.

5.2 Drop-rotation start-up

The velocity development of a levitated drop under an applied steady torque is shown in Fig. 7. It can be seen that the shear stress due to the applied torque initially drives fluids in vicinity of the drop surface. The viscous stress gradually spreads towards the center of the drop and acts throughout. Then, the drop begins to rotate about its center. As expected, the rotational velocity of the liquid drop increases under the steady torque; however, for $t > 20\tau$, the

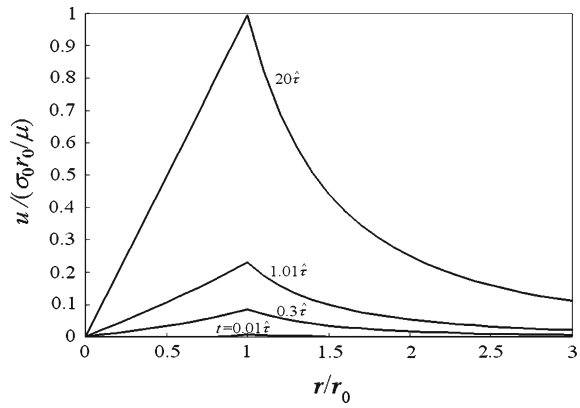

Fig. 7 Velocity field in a rotating water drop and the surrounding region with constant interfacial shear stress $\sigma_0 \sin\theta$ in an infinite medium

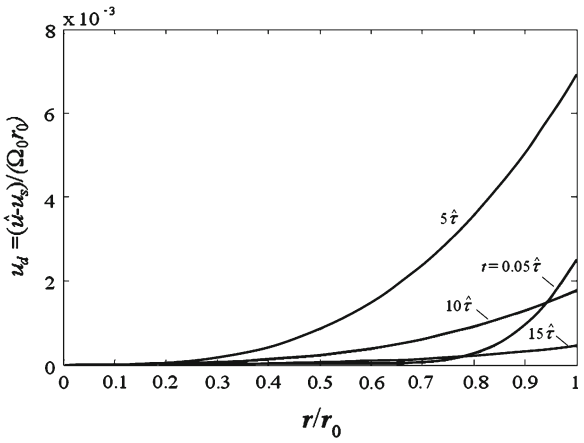

Fig. 8 Liquid-velocity deviation $u_d = (\hat{u} - u_s)/(\Omega_0 r_0)$ from the asymptotic center-point velocity (steady torque start-up)

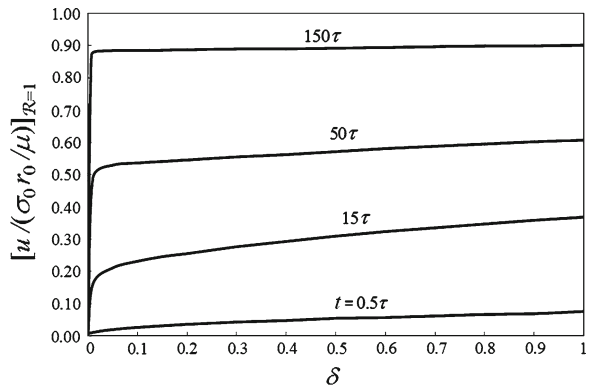

Fig. 9 Dimensionless interfacial velocity as a function of the viscosity ratio δ for it $\lambda = 0.001$ at various times (steady torque start-up)

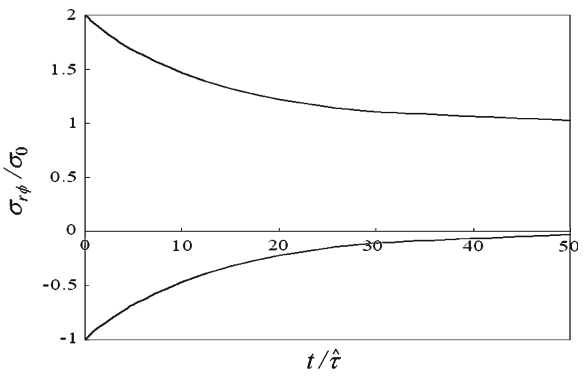

Fig. 10 Tangential stresses at the surface of a water drop under a steady torque

rotation eventually comes quite close to the steady state and the liquid drop steadily rotates like a solid body with a constant rotation rate. In order to amplify the liquid-region velocity, the asymptotic velocity as $r \to 0$ is subtracted, and the resulting dimessionless velocity $u_d = (\hat{u} - u_s)/(\Omega_0 r_0)$ is plotted in Fig. 8. Unlike the decelerating-drop case, $(\hat{u} - u_s)$ is not divided by u_s for scaling because u_s is very nearly zero at very early times. In Fig. 9, the interfacial velocity is plotted as a function of the viscosity ratio δ for a fixed density ratio $\lambda = 0.001$ at various times. The results show a steady increase of the interfacial velocity with increasing δ.

The scaled interfacial shear stress is plotted in Fig. 10 against scaled time. Note that the sign of the shear stress in the plot indicates only the direction of shear stress. The result shows that the shear stress decreases gradually after the applied torque is exerted on the drop surface. It is consistent with the velocity development shown above; indeed, the interfacial stress at the liquid side vanishes as the drop rotates like a solid body in steady state. In this state, the applied shear stress on the drop surface is taken up entirely by the motion of the gas, and the liquid drop is able to maintain a steady solid-body rotation.

For the solid-sphere case, when turning on the torque, the sphere starts to rotate about its axis as expected. For a density ratio $\lambda = 0.0012$, the development of the velocity induced by the rotating sphere is shown in Fig. 11. As one might anticipate from the results, the sphere, as well as the induced flow field, will reach a steady state and the applied shear stress is entirely taken up by the fluid motion.

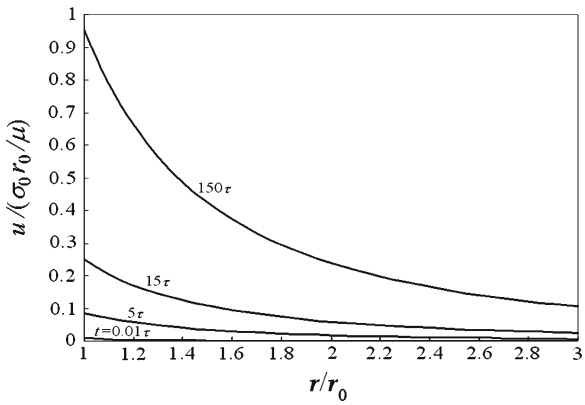

Fig. 11 Velocity field in a gaseous medium induced by a rotating solid sphere under a steady shear stress σ_0 sin θ ($\lambda = 0.0012$)

As in the decelerating-drop case, we have provided a plot of the interfacial velocity as a continuous function of the viscosity ratio δ for various values of time and fixed density ratio λ. For short times, a steady and gentle decrease of the interfacial velocity with increasing viscosity ratio is seen. For large times, the decrease is quite sharp.

6 Conclusions

The transient dynamics of a rotating drop has been studied in the limit of the low-Reynolds-number approximation. The results show that the transient effect initially takes place at the drop surface when the applied torque is either turned on or off. The transient effect will gradually spread into the drop inside and vanish eventually. The maximum deviation of the drop-velocity distribution from the solid-body velocity takes place at the drop surface. However, the deviation depends on the viscosity of the liquid drop. For highly viscous liquids, the velocity deviation is relatively small, especially away from the drop surface. Therefore, for the liquids under consideration, turning the applied torque on or off will affect the velocity field of the rotating drop very little and it is reasonable to approximate the bulk of the drop motion by a solid-body rotation. For short times (order of $0 - 0.3\tau$) soon after start-up or slow down, the stress on the surface of the drop may not be negligible.

Acknowledgments A scholarship from the Ministry of Science and Technology of the Royal Thai Government for one of us (CA) is gratefully acknowledged.

Appendix A: Relevant inverse Laplace transforms

$$\mathsf{L}^{-1}\left[\frac{\mathrm{e}^{-zx}}{s}\right] = \operatorname{erfc}\left(\frac{x}{2(at)^{1/2}}\right), \tag{A.1}$$

$$\mathsf{L}^{-1}\left[\frac{\mathrm{e}^{-zx}}{s(z+k)}\right] = \frac{1}{k}\operatorname{erfc}\left(\frac{x}{2(at)^{1/2}}\right) - \frac{1}{k}\mathrm{e}^{kx+ak^2t}\operatorname{erfc}\left(\frac{x}{2(at)^{1/2}} + k(at)^{1/2}\right), \tag{A.2}$$

$$\mathsf{L}^{-1}\left[\frac{\mathrm{e}^{-zx}}{s(z+k)^2}\right] = \frac{1}{k^2}\operatorname{erfc}\left(\frac{x}{2(at)^{1/2}}\right) - \frac{2}{k}\left(\frac{at}{\pi}\right)^{1/2} \times \mathrm{e}^{-x^2/4at} - \frac{1}{k^2}(1 - kx - 2ak^2t)\operatorname{erfc}\left(\frac{x}{2(at)^{1/2}} + k(at)^{1/2}\right)\mathrm{e}^{kx+ak^2t}, \tag{A.3}$$

where, $z = (s/a)^{1/2}$; a and x are positive real while k may be complex. The values of k are given by the various roots of the cubic polynomial in the denominator of the term $G(r, s)$ in (8) and (9), as well as $\Omega(s)$in (10b).

The expressions for the individual real and imaginary components of the roots a_m, b_m, c_m are given in Appendix C. Other inverse Laplace transforms involving these parameters are given in Appendix B.

Appendix B: Expressions for I_n^0, I_n^1, $\hat{J}_n^0$ and $\hat{J}_n^1$

$$\hat{I}_1^0 = -2\left\{\frac{a_1a_3+b_1b_3}{a_1^2+b_1^2}\operatorname{erfc}\left(\frac{1-\mathsf{R}}{\sqrt{4t/\hat{\tau}}}\right) - \left[\frac{a_1a_3+b_1b_3}{a_1^2+b_1^2}\cos\theta_1 - \frac{a_1b_3-b_1a_3}{a_1^2+b_1^2}\sin\theta_1\right]\Sigma_1 \mathrm{e}^{(1-\mathsf{R})a_1+(a_1^2-b_1^2)\frac{t}{\hat{\tau}}}\right\},$$

$$\hat{I}_2^0 = -\frac{c_3}{c_1}\left\{\operatorname{erfc}\left(\frac{1-\mathsf{R}}{\sqrt{4t/\hat{\tau}}}\right) - \mathrm{e}^{c_1(1-\mathsf{R})+c_1^2\frac{t}{\hat{\tau}}}\operatorname{erfc}\left(\frac{1-\mathsf{R}}{\sqrt{4t/\hat{\tau}}}+c_1\sqrt{t/\hat{\tau}}\right)\right\},$$

$$\hat{I}_3^0 = 2\left\{\frac{a_1a_4+b_1b_4}{a_1^2+b_1^2}\operatorname{erfc}\left(\frac{1+\mathsf{R}}{\sqrt{4t/\hat{\tau}}}\right) - \left[\frac{a_1a_4+b_1b_4}{a_1^2+b_1^2}\cos\theta_2 - \frac{a_1b_4-b_1a_4}{a_1^2+b_1^2}\sin\theta_2\right]\Sigma_2 \mathrm{e}^{(1+\mathsf{R})a_1+(a_1^2-b_1^2)\frac{t}{\hat{\tau}}}\right\},$$

$$\hat{I}_4^0 = \frac{c_4}{c_1}\left\{\operatorname{erfc}\left(\frac{1+\mathsf{R}}{\sqrt{4t/\hat{\tau}}}\right) - \mathrm{e}^{c_1(1+\mathsf{R})+c_1^2\frac{t}{\hat{\tau}}}\operatorname{erfc}\left(\frac{1+\mathsf{R}}{\sqrt{4t/\hat{\tau}}}+c_1\sqrt{t/\hat{\tau}}\right)\right\},$$

$$\hat{I}_1^1 = -2\left\{\frac{a_1a_5+b_1b_5}{a_1^2+b_1^2}\operatorname{erfc}\left(\frac{3-\mathsf{R}}{\sqrt{4t/\hat{\tau}}}\right) - \left[\frac{a_1a_5+b_1b_5}{a_1^2+b_1^2}\cos\theta_3 - \frac{a_1b_5-b_1a_5}{a_1^2+b_1^2}\sin\theta_3\right]\Sigma_3 \mathrm{e}^{(3-\mathsf{R})a_1+(a_1^2-b_1^2)\frac{t}{\hat{\tau}}}\right\},$$

$$\hat{I}_2^1 = -\frac{c_5}{c_1}\left\{\operatorname{erfc}\left(\frac{3-\mathsf{R}}{\sqrt{4t/\hat{\tau}}}\right) - \mathrm{e}^{c_1(3-\mathsf{R})+c_1^2\frac{t}{\hat{\tau}}}\operatorname{erfc}\left(\frac{3-\mathsf{R}}{\sqrt{4t/\hat{\tau}}}+c_1\sqrt{t/\hat{\tau}}\right)\right\},$$

$$\begin{aligned}\hat{I}_3^1 = -2\Bigg\{&\frac{(a_1^2-b_1^2)a_6+2a_1b_1b_6}{(a_1^2+b_1^2)^2}\operatorname{erfc}\left(\frac{3-\mathsf{R}}{\sqrt{4t/\hat{\tau}}}\right) - \frac{a_1a_6+b_1b_6}{a_1^2+b_1^2}\sqrt{\frac{4t}{\pi\hat{\tau}}}\mathrm{e}^{-\frac{(3-\mathsf{R})^2\hat{\tau}}{4t}}\\ &+\left(b_6\left[\frac{a_1^2-b_1^2}{(a_1^2+b_1^2)^2} - \frac{a_1(3-\mathsf{R})}{a_1^2+b_1^2} - 2\frac{t}{\hat{\tau}}\right] + a_6\left[\frac{a_1(3-\mathsf{R})}{a_1^2+b_1^2} - \frac{2a_1b_1}{(a_1^2+b_1^2)^2}\right]\right)\Sigma_3 \mathrm{e}^{(3-\mathsf{R})a_1+(a_1^2-b_1^2)\frac{t}{\hat{\tau}}}\sin\theta_3\Bigg\},\end{aligned}$$

$$\hat{I}_4^1 = -\frac{c_6}{c_1^2}\left\{\operatorname{erfc}\left(\frac{3-\mathsf{R}}{\sqrt{4t/\hat{\tau}}}\right) - c_1\sqrt{\frac{4t}{\pi\hat{\tau}}}\mathrm{e}^{-\frac{(3-\mathsf{R})^2\hat{\tau}}{4t}} - \left[1-c_1(3-\mathsf{R})-\frac{2c_1^2t}{\hat{\tau}}\right]\mathrm{e}^{c_1(3-\mathsf{R})+\frac{c_1^2t}{\hat{\tau}}}\operatorname{erfc}\left(\frac{3-\mathsf{R}}{\sqrt{4t/\hat{\tau}}}+c_1\sqrt{t/\hat{\tau}}\right)\right\},$$

$$\hat{I}_5^1 = 2\left\{\frac{a_1a_7+b_1b_7}{a_1^2+b_1^2}\operatorname{erfc}\left(\frac{3+\mathsf{R}}{\sqrt{4t/\hat{\tau}}}\right) - \left[\frac{a_1a_7+b_1b_7}{a_1^2+b_1^2}\cos\theta_4 - \frac{a_1b_7-b_1a_7}{a_1^2+b_1^2}\sin\theta_4\right]\Sigma_4 \mathrm{e}^{(3+\mathsf{R})a_1+(a_1^2-b_1^2)\frac{t}{\hat{\tau}}}\right\},$$

$$\hat{I}_6^1 = \frac{c_7}{c_1}\left\{\operatorname{erfc}\left(\frac{3+\mathsf{R}}{\sqrt{4t/\hat{\tau}}}\right) - \mathrm{e}^{c_1(3+\mathsf{R})+c_1^2\frac{t}{\hat{\tau}}}\operatorname{erfc}\left(\frac{3+\mathsf{R}}{\sqrt{4t/\hat{\tau}}}+c_1\sqrt{t/\hat{\tau}}\right)\right\},$$

$$\begin{aligned}\hat{I}_7^1 = 2\Bigg\{&\frac{(a_1^2-b_1^2)a_8+2a_1b_1b_8}{(a_1^2+b_1^2)^2}\operatorname{erfc}\left(\frac{3+\mathsf{R}}{\sqrt{4t/\hat{\tau}}}\right) - \frac{a_1a_8+b_1b_8}{a_1^2+b_1^2}\sqrt{\frac{4t}{\pi\hat{\tau}}}\mathrm{e}^{-\frac{(3+\mathsf{R})^2\hat{\tau}}{4t}}\\ &-\left(a_8\left[\frac{a_1^2-b_1^2}{(a_1^2+b_1^2)^2} - \frac{a_1(3+\mathsf{R})}{a_1^2+b_1^2} - 2\frac{t}{\hat{\tau}}\right] - b_8\left[\frac{a_1(3+\mathsf{R})}{a_1^2+b_1^2} - \frac{2a_1b_1}{(a_1^2+b_1^2)^2}\right]\right)\Sigma_4 \mathrm{e}^{(3+\mathsf{R})a_1+(a_1^2-b_1^2)\frac{t}{\hat{\tau}}}\cos\theta_4\\ &+\left(b_8\left[\frac{a_1^2-b_1^2}{(a_1^2+b_1^2)^2} - \frac{a_1(3+\mathsf{R})}{a_1^2+b_1^2} - 2\frac{t}{\hat{\tau}}\right] + a_8\left[\frac{a_1(3+\mathsf{R})}{a_1^2+b_1^2} - \frac{2a_1b_1}{(a_1^2+b_1^2)^2}\right]\right)\Sigma_4 \mathrm{e}^{(3+\mathsf{R})a_1+(a_1^2-b_1^2)\frac{t}{\hat{\tau}}}\sin\theta_4\Bigg\},\end{aligned}$$

$$\hat{I}_8^1 = \frac{c_8}{c_1^2}\left\{\operatorname{erfc}\left(\frac{3+\mathsf{R}}{\sqrt{4t/\hat{\tau}}}\right) - c_1\sqrt{\frac{4t}{\pi\hat{\tau}}}\mathrm{e}^{-\frac{(3+\mathsf{R})^2\hat{\tau}}{4t}} - \left[1-c_1(3+\mathsf{R})-\frac{2c_1^2t}{\hat{\tau}}\right]\mathrm{e}^{c_1(3+\mathsf{R})+\frac{c_1^2t}{\hat{\tau}}}\operatorname{erfc}\left(\frac{3+\mathsf{R}}{\sqrt{4t/\hat{\tau}}}+c_1\sqrt{t/\hat{\tau}}\right)\right\},$$

where

$$\Sigma_k = \text{abs}\left\{\text{erfc}\left(\frac{1+(-1)^k\mathsf{R}}{\sqrt{4t/\hat{\tau}}} + (a_1+b_1 i)\sqrt{t/\hat{\tau}}\right)\right\}, \quad \text{for } k = 1, 2,$$

$$\Sigma_k = \text{abs}\left\{\text{erfc}\left(\frac{3+(-1)^k\mathsf{R}}{\sqrt{4t/\hat{\tau}}} + (a_1+b_1 i)\sqrt{t/\hat{\tau}}\right)\right\}, \quad \text{for } k = 3, 4,$$

$$\theta_k = b_1[1+(-1)^k R] + 2a_1 b_1 \frac{t}{\hat{\tau}} + \arg\left\{\text{erfc}\left(\frac{1+(-1)^k\mathsf{R}}{\sqrt{4t/\hat{\tau}}} + (a_1+b_1 i)\sqrt{t/\hat{\tau}}\right)\right\}, \quad \text{for } k = 1, 2,$$

$$\theta_k = b_1[3+(-1)^k R] + 2a_1 b_1 \frac{t}{\hat{\tau}} + \arg\left\{\text{erfc}\left(\frac{3+(-1)^k\mathsf{R}}{\sqrt{4t/\hat{\tau}}} + (a_1+b_1 i)\sqrt{t/\hat{\tau}}\right)\right\}, \quad \text{for } k = 3, 4,$$

and $\mathsf{R} = (r/r_0)$ is the dimensionless radial coordinate.

The coefficients a_m, b_m, and c_m, are given in Appendix C.

$$I_1^0 = -2\left\{\frac{a_1a_3+b_1b_3}{a_1^2+b_1^2}\text{erfc}\left(\frac{2+\kappa(\mathsf{R}-1)}{\sqrt{4t/\hat{\tau}}}\right) - \left[\frac{a_1a_3+b_1b_3}{a_1^2+b_1^2}\cos\theta_1 - \frac{a_1b_3-b_1a_3}{a_1^2+b_1^2}\sin\theta_1\right]\Sigma_1 \text{e}^{[2+\kappa(\mathsf{R}-1)]a_1+(a_1^2-b_1^2)\frac{t}{\hat{\tau}}}\right\},$$

$$I_2^0 = -\frac{c_3}{c_1}\left\{\text{erfc}\left(\frac{2+\kappa(\mathsf{R}-1)}{\sqrt{4t/\hat{\tau}}}\right) - \text{e}^{[2+\kappa(\mathsf{R}-1)]c_1+c_1^2\frac{t}{\hat{\tau}}}\text{erfc}\left(\frac{2+\kappa(\mathsf{R}-1)}{\sqrt{4t/\hat{\tau}}} + c_1\sqrt{t/\hat{\tau}}\right)\right\},$$

$$I_3^0 = 2\left\{\frac{a_1a_4+b_1b_4}{a_1^2+b_1^2}\text{erfc}\left(\frac{\kappa(\mathsf{R}-1)}{\sqrt{4t/\hat{\tau}}}\right) - \left[\frac{a_1a_4+b_1b_4}{a_1^2+b_1^2}\cos\theta_2 - \frac{a_1b_4-b_1a_4}{a_1^2+b_1^2}\sin\theta_2\right]\Sigma_2 \text{e}^{\kappa(\mathsf{R}-1)a_1+(a_1^2-b_1^2)\frac{t}{\hat{\tau}}}\right\},$$

$$I_4^0 = \frac{c_4}{c_1}\left\{\text{erfc}\left(\frac{\kappa(\mathsf{R}-1)}{\sqrt{4t/\hat{\tau}}}\right) - \text{e}^{\kappa(\mathsf{R}-1)c_1+c_1^2\frac{t}{\hat{\tau}}}\text{erfc}\left(\frac{\kappa(\mathsf{R}-1)}{\sqrt{4t/\hat{\tau}}} + c_1\sqrt{t/\hat{\tau}}\right)\right\},$$

$$I_1^1 = -2\left\{\frac{a_1a_5+b_1b_5}{a_1^2+b_1^2}\text{erfc}\left(\frac{4+\kappa(\mathsf{R}-1)}{\sqrt{4t/\hat{\tau}}}\right) - \left[\frac{a_1a_5+b_1b_5}{a_1^2+b_1^2}\cos\theta_3 - \frac{a_1b_5-b_1a_5}{a_1^2+b_1^2}\sin\theta_3\right]\Sigma_3 \text{e}^{[4+\kappa(\mathsf{R}-1)]a_1+(a_1^2-b_1^2)\frac{t}{\hat{\tau}}}\right\},$$

$$I_2^1 = -\frac{c_5}{c_1}\left\{\text{erfc}\left(\frac{4+\kappa(\mathsf{R}-1)}{\sqrt{4t/\hat{\tau}}}\right) - \text{e}^{[4+\kappa(\mathsf{R}-1)]c_1+c_1^2\frac{t}{\hat{\tau}}}\text{erfc}\left(\frac{4+\kappa(\mathsf{R}-1)}{\sqrt{4t/\hat{\tau}}} + c_1\sqrt{t/\hat{\tau}}\right)\right\},$$

$$I_3^1 = -2\left\{\frac{(a_1^2-b_1^2)a_6+2a_1b_1b_6}{(a_1^2+b_1^2)^2}\text{erfc}\left(\frac{4+\kappa(\mathsf{R}-1)}{\sqrt{4t/\hat{\tau}}}\right) - \frac{a_1a_6+b_1b_6}{a_1^2+b_1^2}\sqrt{\frac{4t}{\pi\hat{\tau}}}\text{e}^{-\frac{[4+\kappa(\mathsf{R}-1)]^2\hat{\tau}}{4t}} + \right.$$

$$- \left(a_6\left[\frac{a_1^2-b_1^2}{(a_1^2+b_1^2)^2} - \frac{[4+\kappa(\mathsf{R}-1)]a_1}{a_1^2+b_1^2} - 2\frac{t}{\hat{\tau}}\right] - b_6\left[\frac{[4+\kappa(\mathsf{R}-1)]a_1}{a_1^2+b_1^2} - \frac{2a_1b_1}{(a_1^2+b_1^2)^2}\right]\right)\Sigma_3 \text{e}^{[4+\kappa(\mathsf{R}-1)]a_1+(a_1^2-b_1^2)\frac{t}{\hat{\tau}}}\cos\theta_3$$

$$\left. + \left(b_6\left[\frac{a_1^2-b_1^2}{(a_1^2+b_1^2)^2} - \frac{[4+\kappa(\mathsf{R}-1)]a_1}{a_1^2+b_1^2} - 2\frac{t}{\hat{\tau}}\right] + a_6\left[\frac{[4+\kappa(\mathsf{R}-1)]a_1}{a_1^2+b_1^2} - \frac{2a_1b_1}{(a_1^2+b_1^2)^2}\right]\right)\Sigma_3 \text{e}^{[4+\kappa(\mathsf{R}-1)]a_1+(a_1^2-b_1^2)\frac{t}{\hat{\tau}}}\sin\theta_3\right\},$$

$$I_4^1 = -\frac{c_6}{c_1^2}\left\{\text{erfc}\left(\frac{4+\kappa(\mathsf{R}-1)}{\sqrt{4t/\hat{\tau}}}\right) - c_1\sqrt{\frac{4t}{\pi\hat{\tau}}}\text{e}^{-\frac{[4+\kappa(\mathsf{R}-1)]^2\hat{\tau}}{4t}} - \left[1-[4+\kappa(\mathsf{R}-1)]c_1 - \frac{2c_1^2t}{\hat{\tau}}\right]\text{e}^{[4+\kappa(\mathsf{R}-1)]c_1+\frac{c_1^2t}{\hat{\tau}}}\right.$$

$$\left.\times\text{erfc}\left(\frac{4+\kappa(\mathsf{R}-1)}{\sqrt{4t/\hat{\tau}}} + c_1\sqrt{t/\hat{\tau}}\right)\right\},$$

$$I_5^1 = 2\left\{\frac{a_1a_7+b_1b_7}{a_1^2+b_1^2}\text{erfc}\left(\frac{2+\kappa(\mathsf{R}-1)}{\sqrt{4t/\hat{\tau}}}\right) - \left[\frac{a_1a_7+b_1b_7}{a_1^2+b_1^2}\cos\theta_4 - \frac{a_1b_7-b_1a_7}{a_1^2+b_1^2}\sin\theta_4\right]\Sigma_4 \text{e}^{[2+\kappa(\mathsf{R}-1)]a_1+(a_1^2-b_1^2)\frac{t}{\hat{\tau}}}\right\},$$

$$I_6^1 = \frac{c_7}{c_1}\left\{\operatorname{erfc}\left(\frac{2+\kappa(\mathsf{R}-1)}{\sqrt{4t/\hat{\tau}}}\right) - \mathrm{e}^{[2+\kappa(\mathsf{R}-1)]c_1+c_1^2\frac{t}{\hat{\tau}}}\operatorname{erfc}\left(\frac{2+\kappa(\mathsf{R}-1)}{\sqrt{4t/\hat{\tau}}}+c_1\sqrt{t/\hat{\tau}}\right)\right\},$$

$$I_7^1 = 2\left\{\frac{(a_1^2-b_1^2)a_8+2a_1b_1b_8}{(a_1^2+b_1^2)^2}\operatorname{erfc}\left(\frac{2+\kappa(\mathsf{R}-1)}{\sqrt{4t/\hat{\tau}}}\right) - \frac{a_1a_8+b_1b_8}{a_1^2+b_1^2}\sqrt{\frac{4t}{\pi\hat{\tau}}}\mathrm{e}^{-\frac{[2+\kappa(\mathsf{R}-1)]^2\hat{\tau}}{4t}}+\right.$$
$$-\left(a_8\left[\frac{a_1^2-b_1^2}{(a_1^2+b_1^2)^2}-\frac{[2+\kappa(\mathsf{R}-1)]a_1}{a_1^2+b_1^2}-2\frac{t}{\hat{\tau}}\right]-b_8\left[\frac{[2+\kappa(\mathsf{R}-1)]a_1}{a_1^2+b_1^2}-\frac{2a_1b_1}{(a_1^2+b_1^2)^2}\right]\right)\Sigma_4\mathrm{e}^{[2+\kappa(\mathsf{R}-1)]a_1+(a_1^2-b_1^2)\frac{t}{\hat{\tau}}}\cos\theta_4$$
$$\left.+\left(b_8\left[\frac{a_1^2-b_1^2}{(a_1^2+b_1^2)^2}-\frac{[2+\kappa(\mathsf{R}-1)]a_1}{a_1^2+b_1^2}-2\frac{t}{\hat{\tau}}\right]+a_8\left[\frac{[2+\kappa(\mathsf{R}-1)]a_1}{a_1^2+b_1^2}-\frac{2a_1b_1}{(a_1^2+b_1^2)^2}\right]\right)\Sigma_4\mathrm{e}^{[2+\kappa(\mathsf{R}-1)]a_1+(a_1^2-b_1^2)\frac{t}{\hat{\tau}}}\sin\theta_4\right\},$$

$$I_8^1 = \frac{c_8}{c_1^2}\left\{\operatorname{erfc}\left(\frac{2+\kappa(\mathsf{R}-1)}{\sqrt{4t/\hat{\tau}}}\right) - c_1\sqrt{\frac{4t}{\pi\hat{T}}}\mathrm{e}^{-\frac{[2+\kappa(\mathsf{R}-1)]^2\hat{\tau}}{4t}} - \left[1-[2+\kappa(\mathsf{R}-1)]c_1\right.\right.$$
$$\left.\left.-\frac{2c_1^2t}{\hat{\tau}}\right]\mathrm{e}^{[2+\kappa(\mathsf{R}-1)]c_1+\frac{c_1^2t}{\hat{\tau}}}\operatorname{erfc}\left(\frac{2+\kappa(\mathsf{R}-1)}{\sqrt{4t/\hat{\tau}}}+c_1\sqrt{t/\hat{\tau}}\right)\right\},$$

$$\hat{J}_1^0 = 2\left\{\frac{a_1a_9+b_1b_9}{a_1^2+b_1^2}\operatorname{erfc}\left(\frac{1-\mathsf{R}}{\sqrt{4t/\hat{\tau}}}\right) - \left[\frac{a_1a_9+b_1b_9}{a_1^2+b_1^2}\cos\theta_1 - \frac{a_1b_9-b_1a_9}{a_1^2+b_1^2}\sin\theta_1\right]\Sigma_1\mathrm{e}^{(1-\mathsf{R})a_1+(a_1^2-b_1^2)\frac{t}{\hat{\tau}}}\right\},$$

$$\hat{J}_2^0 = -\operatorname{erfc}\left(\frac{1-\mathsf{R}}{\sqrt{4t/\hat{\tau}}}\right) + \frac{c_9}{c_1}\left\{\operatorname{erfc}\left(\frac{1-\mathsf{R}}{\sqrt{4t/\hat{\tau}}}\right) - \mathrm{e}^{c_1(1-\mathsf{R})+c_1^2\frac{t}{\hat{\tau}}}\operatorname{erfc}\left(\frac{1-\mathsf{R}}{\sqrt{4t/\hat{\tau}}}+c_1\sqrt{t/\hat{\tau}}\right)\right\},$$

$$\hat{J}_3^0 = -2\left\{\frac{a_1a_{10}+b_1b_{10}}{a_1^2+b_1^2}\operatorname{erfc}\left(\frac{1+\mathsf{R}}{\sqrt{4t/\hat{\tau}}}\right) - \left[\frac{a_1a_{10}+b_1b_{10}}{a_1^2+b_1^2}\cos\theta_2 - \frac{a_1b_{10}-b_1a_{10}}{a_1^2+b_1^2}\sin\theta_2\right]\Sigma_2\mathrm{e}^{(1+\mathsf{R})a_1+(a_1^2-b_1^2)\frac{t}{\hat{\tau}}}\right\},$$

$$\hat{J}_4^0 = \operatorname{erfc}\left(\frac{1-\mathsf{R}}{\sqrt{4t/\hat{\tau}}}\right) - \frac{c_{10}}{c_1}\left\{\operatorname{erfc}\left(\frac{1+\mathsf{R}}{\sqrt{4t/\hat{\tau}}}\right) - \mathrm{e}^{c_1(1+\mathsf{R})+c_1^2\frac{t}{\hat{\tau}}}\operatorname{erfc}\left(\frac{1+\mathsf{R}}{2\sqrt{t/\hat{\tau}}}+c_1\sqrt{t/\hat{\tau}}\right)\right\},$$

$$\hat{J}_1^1 = 2\left\{\frac{a_1a_{11}+b_1b_{11}}{a_1^2+b_1^2}\operatorname{erfc}\left(\frac{3-\mathsf{R}}{\sqrt{4t/\hat{\tau}}}\right) - \left[\frac{a_1a_{11}+b_1b_{11}}{a_1^2+b_1^2}\cos\theta_3 - \frac{a_1b_{11}-b_1a_{11}}{a_1^2+b_1^2}\sin\theta_3\right]\Sigma_3\mathrm{e}^{(3-\mathsf{R})a_1+(a_1^2-b_1^2)\frac{t}{\hat{\tau}}}\right\},$$

$$\hat{J}_2^1 = -\operatorname{erfc}\left(\frac{3-\mathsf{R}}{\sqrt{4t/\hat{\tau}}}\right) + \frac{c_{11}}{c_1}\left\{\operatorname{erfc}\left(\frac{3-\mathsf{R}}{\sqrt{4t/\hat{\tau}}}\right) - \mathrm{e}^{c_1(3-\mathsf{R})+c_1^2\frac{t}{\hat{\tau}}}\operatorname{erfc}\left(\frac{3-\mathsf{R}}{\sqrt{4t/\hat{\tau}}}+c_1\sqrt{t/\hat{\tau}}\right)\right\},$$

$$\hat{J}_3^1 = 2\left\{\frac{(a_1^2-b_1^2)a_{12}+2a_1b_1b_{12}}{(a_1^2+b_1^2)^2}\operatorname{erfc}\left(\frac{3-\mathsf{R}}{\sqrt{4t/\hat{\tau}}}\right) - \frac{a_1a_{12}+b_1b_{12}}{a_1^2+b_1^2}\sqrt{\frac{4t}{\pi\hat{\tau}}}\mathrm{e}^{-\frac{(3-\mathsf{R})^2\hat{\tau}}{4t}}+\right.$$
$$-\left(a_{12}\left[\frac{a_1^2-b_1^2}{(a_1^2+b_1^2)^2}-\frac{a_1(3-\mathsf{R})}{a_1^2+b_1^2}-2\frac{t}{\hat{\tau}}\right]-b_{12}\left[\frac{a_1(3-\mathsf{R})}{a_1^2+b_1^2}-\frac{2a_1b_1}{(a_1^2+b_1^2)^2}\right]\right)\Sigma_3\mathrm{e}^{(3-\mathsf{R})a_1+(a_1^2-b_1^2)\frac{t}{\hat{\tau}}}\cos\theta_3+$$
$$\left.+\left(b_{12}\left[\frac{a_1^2-b_1^2}{(a_1^2+b_1^2)^2}-\frac{a_1(3-\mathsf{R})}{a_1^2+b_1^2}-2\frac{t}{\hat{\tau}}\right]+a_{12}\left[\frac{a_1(3-\mathsf{R})}{a_1^2+b_1^2}-\frac{2a_1b_1}{(a_1^2+b_1^2)^2}\right]\right)\Sigma_3\mathrm{e}^{(3-\mathsf{R})a_1+(a_1^2-b_1^2)\frac{t}{\hat{\tau}}}\sin\theta_3\right\},$$

$$\hat{J}_4^1 = \frac{c_{12}}{c_1^2}\left\{\operatorname{erfc}\left(\frac{3-\mathsf{R}}{\sqrt{4t/\hat{\tau}}}\right) - c_1\sqrt{\frac{4t}{\pi\hat{\tau}}}\mathrm{e}^{-\frac{(3-\mathsf{R})^2\hat{\tau}}{4t}} - \left[1-c_1(3-\mathsf{R})-\frac{2c_1^2t}{\hat{\tau}}\right]\mathrm{e}^{c_1(3-\mathsf{R})+\frac{c_1^2t}{\hat{\tau}}}\operatorname{erfc}\left(\frac{3-\mathsf{R}}{\sqrt{4t/\hat{\tau}}}+c_1\sqrt{t/\hat{\tau}}\right)\right\}$$
$$-\operatorname{erfc}\left(\frac{3-\mathsf{R}}{\sqrt{4t/\hat{\tau}}}\right),$$

$$\hat{J}_5^1 = -2\left\{\frac{a_1a_{13}+b_1b_{13}}{a_1^2+b_1^2}\operatorname{erfc}\left(\frac{3+\mathsf{R}}{\sqrt{4t/\hat{\tau}}}\right) - \left[\frac{a_1a_{13}+b_1b_{13}}{a_1^2+b_1^2}\cos\theta_4 - \frac{a_1b_{13}-b_1a_{13}}{a_1^2+b_1^2}\sin\theta_4\right]\Sigma_4\mathrm{e}^{(3+\mathsf{R})a_1+(a_1^2-b_1^2)\frac{t}{\hat{\tau}}}\right\},$$

$$\hat{J}_6^1 = \operatorname{erfc}\left(\frac{3+\mathsf{R}}{\sqrt{4t/\hat{\tau}}}\right) - \frac{c_{13}}{c_1}\left\{\operatorname{erfc}\left(\frac{3+\mathsf{R}}{\sqrt{4t/\hat{\tau}}}\right) - \mathrm{e}^{c_1(3+\mathsf{R})+c_1^2\frac{t}{\hat{\tau}}}\operatorname{erfc}\left(\frac{3+\mathsf{R}}{\sqrt{4t/\hat{\tau}}} + c_1\sqrt{t/\hat{\tau}}\right)\right\},$$

$$\begin{aligned}\hat{J}_7^1 = -2\Bigg\{ & \frac{(a_1^2-b_1^2)a_{14}+2a_1b_1b_{14}}{(a_1^2+b_1^2)^2}\operatorname{erfc}\left(\frac{3+\mathsf{R}}{\sqrt{4t/\hat{\tau}}}\right) - \frac{a_1a_{14}+b_1b_{14}}{a_1^2+b_1^2}\sqrt{\frac{4t}{\pi\hat{\tau}}}\mathrm{e}^{-\frac{(3+\mathsf{R})^2\hat{\tau}}{4t}} + \\ & -\left(a_{14}\left[\frac{a_1^2-b_1^2}{(a_1^2+b_1^2)^2} - \frac{a_1(3+\mathsf{R})}{a_1^2+b_1^2} - 2\frac{t}{\hat{\tau}}\right] - b_{14}\left[\frac{a_1(3+\mathsf{R})}{a_1^2+b_1^2} - \frac{2a_1b_1}{(a_1^2+b_1^2)^2}\right]\right)\Sigma_4\mathrm{e}^{(3+\mathsf{R})a_1+(a_1^2-b_1^2)\frac{t}{\hat{\tau}}}\cos\theta_4 \\ & +\left(b_{14}\left[\frac{a_1^2-b_1^2}{(a_1^2+b_1^2)^2} - \frac{a_1(3+\mathsf{R})}{a_1^2+b_1^2} - 2\frac{t}{\hat{\tau}}\right] + a_{14}\left[\frac{a_1(3+\mathsf{R})}{a_1^2+b_1^2} - \frac{2a_1b_1}{(a_1^2+b_1^2)^2}\right]\right)\Sigma_4\mathrm{e}^{(3+\mathsf{R})a_1+(a_1^2-b_1^2)\frac{t}{\hat{\tau}}}\sin\theta_4\Bigg\},\end{aligned}$$

$$\begin{aligned}\hat{J}_8^1 = -\frac{c_{14}}{c_1^2}\Bigg\{ & \operatorname{erfc}\left(\frac{3+\mathsf{R}}{\sqrt{4t/\hat{\tau}}}\right) - c_1\sqrt{\frac{4t}{\pi\hat{\tau}}}\mathrm{e}^{-\frac{(3+\mathsf{R})^2\hat{\tau}}{4t}} - \left[1 - c_1(3+\mathsf{R}) - \frac{2c_1^2t}{\hat{\tau}}\right]\mathrm{e}^{c_1(3+\mathsf{R})+\frac{c_1^2t}{\hat{\tau}}}\operatorname{erfc}\left(\frac{3+\mathsf{R}}{\sqrt{4t/\hat{\tau}}} + c_1\sqrt{t/\hat{\tau}}\right)\Bigg\} \\ & +\operatorname{erfc}\left(\frac{3+\mathsf{R}}{\sqrt{4t/\hat{\tau}}}\right).\end{aligned}$$

Appendix C: Coefficients a_m, b_m, c_m

The set of the coefficients a_m, b_m and c_m in Appendix B represent various partial-fraction decompositions which are detailed here. The expressions for a_m, b_m, and c_m are given implicitly in terms of the partial fractions because the exact expressions are very complicated. We begin with finding the roots of the cubic functions in $[G(r,s)]^n$(see (8) and (9)):

$$\hat{X}^3 + \frac{c_{12}}{c_{11}}\hat{X}^2 + \frac{c_{13}}{c_{11}}\hat{X} + \frac{c_{14}}{c_{11}} = (\hat{X}-Z_1)(\hat{X}-\bar{Z}_1)(\hat{X}-c_1), \text{ where } Z_1 = a_1 + b_1\mathrm{i} \text{ and } \bar{Z}_1 = a_1 - b_1\mathrm{i},$$

$$\hat{X}^3 + \frac{c_{22}}{c_{21}}\hat{X}^2 + \frac{c_{23}}{c_{21}}\hat{X} + \frac{c_{24}}{c_{21}} = (\hat{X}-Z_2)(\hat{X}-\bar{Z}_2)(\hat{X}-c_2), \text{ where } Z_2 = a_2 + b_2\mathrm{i} \text{ and } \bar{Z}_2 = a_2 - b_2\mathrm{i}.$$

Then, the quotients of the cubic function contained in the series expansion are simplified by partial-fraction expansion. Performing the expansions yields the following results:

for $n = 0$

liquid drop:

$$\begin{aligned}&\frac{\mathrm{e}^{-(1-\mathsf{R})\hat{X}}}{s}\left[\frac{(\kappa\hat{X}+1)(\mathsf{R}\hat{X}-1)}{(\hat{X}-Z_1)(\hat{X}-\bar{Z}_1)(\hat{X}-c_1)}\right] + \frac{\mathrm{e}^{-(1+\mathsf{R})\hat{X}}}{s}\left[\frac{(\kappa\hat{X}+1)(\mathsf{R}\hat{X}+1)}{(\hat{X}-Z_1)(\hat{X}-\bar{Z}_1)(\hat{X}-c_1)}\right] \\ &\quad = \frac{\mathrm{e}^{-(1-\mathsf{R})\hat{X}}}{s}\left[\frac{Z_3}{\hat{X}+Z_1} + \frac{\bar{Z}_3}{\hat{X}+\bar{Z}_1} + \frac{c_3}{\hat{X}+c_1}\right] - \frac{\mathrm{e}^{-(1+\mathsf{R})\hat{X}}}{s}\left[\frac{Z_4}{\hat{X}+Z_1} + \frac{\bar{Z}_4}{\hat{X}+\bar{Z}_1} + \frac{c_4}{\hat{X}+c_1}\right];\end{aligned}$$

gas:

$$\begin{aligned}&\frac{\mathrm{e}^{-(\mathsf{R}-1)\hat{X}}}{s}\left[\frac{(\kappa\mathsf{R}\hat{X}+1)(\hat{X}-1)}{(\hat{X}-Z_1)(\hat{X}-\bar{Z}_1)(\hat{X}-c_1)}\right] + \frac{\mathrm{e}^{-(1+\mathsf{R})X-2\hat{X}}}{s}\left[\frac{(\kappa\mathsf{R}\hat{X}+1)(\hat{X}+1)}{(\hat{X}-Z_1)(\hat{X}-\bar{Z}_1)(\hat{X}-c_1)}\right] \\ &\quad = \frac{\mathrm{e}^{-(\mathsf{R}-1)\hat{X}}}{s}\left[\frac{Z_3}{\hat{X}+Z_1} + \frac{\bar{Z}_3}{\hat{X}+\bar{Z}_1} + \frac{c_3}{\hat{X}+c_1}\right] + \frac{\mathrm{e}^{-(1+\mathsf{R})X-2\hat{X}}}{s}\left[\frac{Z_4}{\hat{X}+Z_1} + \frac{\bar{Z}_4}{\hat{X}+\bar{Z}_1} + \frac{c_4}{\hat{X}+c_1}\right];\end{aligned}$$

Shear stress:

$$\begin{aligned}&\frac{\mathrm{e}^{-\mathsf{R}\hat{X}}}{s}\left[\frac{(\kappa\mathsf{R}\hat{X}+1)(\mathsf{R}^2X^2-3\mathsf{R}X+3)}{(\hat{X}-Z_1)(\hat{X}-\bar{Z}_1)(\hat{X}-c_1)}\right] - \frac{\mathrm{e}^{-\mathsf{R}\hat{X}}}{s}\left[\frac{(\kappa\mathsf{R}\hat{X}+1)(\mathsf{R}^2X^2+3\mathsf{R}X+3)}{(\hat{X}-Z_1)(\hat{X}-\bar{Z}_1)(\hat{X}-c_1)}\right] \\ &\quad = \frac{\mathrm{e}^{-(1-\mathsf{R})\hat{X}}}{s}\left[1 + \frac{Z_9}{\hat{X}+Z_1} + \frac{\bar{Z}_9}{\hat{X}+\bar{Z}_1} + \frac{c_9}{\hat{X}+c_1}\right] - \frac{\mathrm{e}^{-(1+\mathsf{R})\hat{X}}}{s}\left[1 + \frac{Z_{10}}{\hat{X}+Z_1} + \frac{\bar{Z}_{10}}{\hat{X}+\bar{Z}_1} + \frac{c_{10}}{\hat{X}+c_1}\right].\end{aligned}$$

for $n = 1$,
liquid drop:

$$\frac{e^{-(3-R)\hat{X}}}{s}\left[\frac{(\kappa\hat{X}+1)(R\hat{X}-1)(\hat{X}-Z_2)(\hat{X}-\bar{Z}_2)(\hat{X}-c_2)}{(\hat{X}-Z_1)^2(\hat{X}-\bar{Z}_1)^2(\hat{X}-c_1)^2}\right]$$
$$+\frac{e^{-(3+R)\hat{X}}}{s}\left[\frac{(\kappa\hat{X}+1)(R\hat{X}+1)(\hat{X}-Z_2)(\hat{X}-\bar{Z}_2)(\hat{X}-c_2)}{(\hat{X}-Z_1)^2(\hat{X}-\bar{Z}_1)^2(\hat{X}-c_1)^2}\right]$$
$$=\frac{e^{-(3-R)\hat{X}}}{s}\left[1+\frac{Z_5}{\hat{X}+Z_1}+\frac{\bar{Z}_5}{\hat{X}+\bar{Z}_1}+\frac{c_5}{\hat{X}+c_1}+\frac{Z_6}{(\hat{X}+Z_1)^2}+\frac{\bar{Z}_6}{(\hat{X}+\bar{Z}_1)^2}+\frac{c_6}{(\hat{X}+c_1)^2}\right]$$
$$+\frac{e^{-(3+R)\hat{X}}}{s}\left[1+\frac{Z_7}{\hat{X}+Z_1}+\frac{\bar{Z}_7}{\hat{X}+\bar{Z}_1}+\frac{c_7}{\hat{X}+c_1}+\frac{Z_8}{(\hat{X}+Z_1)^2}+\frac{\bar{Z}_8}{(\hat{X}+\bar{Z}_1)^2}+\frac{c_8}{(\hat{X}+c_1)^2}\right];$$

gas:

$$\frac{e^{-(1+R)\hat{X}}}{s}\left[\frac{(\kappa R\hat{X}+1)(\hat{X}-1)(\hat{X}-Z_2)(\hat{X}-\bar{Z}_2)(\hat{X}-c_2)}{(\hat{X}-Z_1)^2(\hat{X}-\bar{Z}_1)^2(\hat{X}-c_1)^2}\right]$$
$$+\frac{e^{-(1+R)\hat{X}-4\hat{X}}}{s}\left[\frac{(\kappa R\hat{X}+1)(\hat{X}+1)(\hat{X}-Z_2)(\hat{X}-\bar{Z}_2)(\hat{X}-c_2)}{(\hat{X}-Z_1)^2(\hat{X}-\bar{Z}_1)^2(\hat{X}-c_1)^2}\right]$$
$$=\frac{e^{-(1+R)\hat{X}}}{s}\left[1+\frac{Z_5}{\hat{X}+Z_1}+\frac{\bar{Z}_5}{\hat{X}+\bar{Z}_1}+\frac{c_5}{\hat{X}+c_1}+\frac{Z_6}{(\hat{X}+Z_1)^2}+\frac{\bar{Z}_6}{(\hat{X}+\bar{Z}_1)^2}+\frac{c_6}{(\hat{X}+c_1)^2}\right]$$
$$+\frac{e^{-(1+R)X-4\hat{X}}}{s}\left[1+\frac{Z_7}{\hat{X}+Z_1}+\frac{\bar{Z}_7}{\hat{X}+\bar{Z}_1}+\frac{c_7}{\hat{X}+c_1}+\frac{Z_8}{(\hat{X}+Z_1)^2}+\frac{\bar{Z}_8}{(\hat{X}+\bar{Z}_1)^2}+\frac{c_8}{(\hat{X}+c_1)^2}\right].$$

Shear stress:

$$\frac{e^{-(2-R)\hat{X}}}{s}\left[\frac{(\kappa R\hat{X}+1)(R^2X^2-3RX+3)(\hat{X}-Z_2)(\hat{X}-\bar{Z}_2)(\hat{X}-c_2)}{(\hat{X}-Z_1)^2(\hat{X}-\bar{Z}_1)^2(\hat{X}-c_1)^2}\right]$$
$$-\frac{e^{-(2+R)\hat{X}}}{s}\left[\frac{(\kappa R\hat{X}+1)(R^2X^2+3RX+3)(\hat{X}-Z_2)(\hat{X}-\bar{Z}_2)(\hat{X}-c_2)}{(\hat{X}-Z_1)^2(\hat{X}-\bar{Z}_1)^2(\hat{X}-c_1)^2}\right]$$
$$=\frac{e^{-(2-R)\hat{X}}}{s}\left[1+\frac{Z_{11}}{\hat{X}+Z_1}+\frac{\bar{Z}_{11}}{\hat{X}+\bar{Z}_1}+\frac{c_{11}}{\hat{X}+c_1}+\frac{Z_{12}}{(\hat{X}+Z_1)^2}+\frac{\bar{Z}_{12}}{(\hat{X}+\bar{Z}_1)^2}+\frac{c_{12}}{(\hat{X}+c_1)^2}\right]$$
$$-\frac{e^{-(2+R)\hat{X}}}{s}\left[1+\frac{Z_{13}}{\hat{X}+Z_1}+\frac{\bar{Z}_{13}}{\hat{X}+\bar{Z}_1}+\frac{c_{13}}{\hat{X}+c_1}+\frac{Z_{14}}{(\hat{X}+Z_1)^2}+\frac{\bar{Z}_{14}}{(\hat{X}+\bar{Z}_1)^2}+\frac{c_{14}}{(\hat{X}+c_1)^2}\right].$$

Here $Z_m = a_m + b_m\mathrm{i}$, $\bar{Z}_m = a_m - b_m\mathrm{i}$ and c_m is a real constant. (minus sign correction made).

It should be noted that the values of the coefficients a_m, b_m, and c_m, $3 \le m \le 8$ in the liquid-drop and gas expressions and $9 \le m \le 14$ in the shear-stress expressions are different, even though the same notations are used in the expressions.

References

1. Asavatesanupap C (2007) Fluid dynamics of a crystallizing particle in a rotating liquid sphere. Ph.D. dissertation, Univesity of Southern California, Los Angeles
2. Chung SK, Trinh EH (1998) Containerless protein crystal growth in rotating levitated drops. J Cryst Growth 194:384–397. doi:10.1016/S0022-0248(98)00542-9

3. Rednikov AY, Riley N, Sadhal SS (2003) The behaviour of a particle in orthogonal acoustic fields. J Fluid Mech 486:1–20. doi:10.1017/S0022112003004312
4. Lamb H (1932) Hydrodynamics. Cambridge University Press, Cambridge
5. Leal LG (1992) Laminar flow and convective transport processes. Butterworth, Boston
6. Ghildyal CD (1960) Unsteady motion of an infinite liquid due to the uniform rotation of a sphere. Quart Appl Math 18(4): 396–399
7. Gradshteyn IS, Ryzhik IM (1965) Table of integrals, series and products. Academic Press, New York
8. Chapra SC, Raymond PC (2006) Numerical methods for engineers. McGraw-Hill Higher Education, Boston